Modeling of Lightning Exposure of Sharp and Blunt Rods

Farouk A. M. Rizk, *Life Fellow, IEEE*

***Abstract*—Corona characteristics of lightning rods exposed to ambient fields due to cloud charges prior to negative leader descent are analyzed, taking into account rod slenderness and relative air density. A new formula is introduced to account for the effect such corona on upward connecting leader initiation. This quantifies the tendency of a sharp lightning rod towards self-shielding, which can be detrimental to the protection of a nearby object, particularly if this object is less susceptible to corona formation. The effect of corona due to cloud charge fields on the attractive radius of a solitary rod is also investigated. Based on discharge physics, the characteristics of a non-self shielding air terminal are then defined. Since large electrodes are susceptible to deteriorating corona performance due to protrusions and water drops, preference is given to a corona-free rod with the smallest diameter, under cloud charge fields. For tall rods or rods exposed to high ambient fields, however, the required diameter of a hemispherically capped rod may be impractical. The physical approach described in this paper satisfactorily accounts for the lightning performance of competing sharp and blunt rods in a previous field investigation.**

***Index Terms*—Corona, leader discharge, lightning protection, lightning rods, space charge.**

I. Introduction

SINCE its invention by Ben Franklin in 1753, the lightning rod has found very wide application and, in general, the experience has been satisfactory [1], [2]. In high voltage power transmission installations, lightning rods have often been supplemented or replaced by overhead ground wires. Although the original notion of discharging clouds by a rod with a sharp tip has been abandoned, the rod shape remained basically unchanged. An excellent review by Standler [3] showed that the controversy between the use of sharp or blunt rods is almost as old as the lightning rod itself. A new look at this question is justified, among other things, by the relatively recent research into the characteristics of long air gaps exposed to slow front electric fields, most notably by Les Renardières Group [4], which placed the conditions for positive leader formation on more solid physical grounds. Other justifications are given below.

The occasional failure of lightning rods to protect nearby objects led some investigators to propose alternative shapes for the air terminal. In 1918, Nicola Tesla [5] criticized the sharp rod and proposed an umbrella-type air terminal with large conducting boundaries.

In 1987, based on high voltage laboratory tests involving positive leaders, G. N. Aleksandrov and G. D. Kadzov [6] also suggested that lightning protection could be made more effective by developing the top surface of the air terminal.

The suggestions of using air terminals with large exposed surfaces, however, did not take into consideration the effect of protrusions, water drops, etc. that are bound to settle on the surface in practical field conditions. In [7], it was shown by positive switching impulse tests on long large-electrode air gaps, that rain could bring the breakdown voltage down to that of a sharp rod, for the same air clearance.

More recently, comparative tests on lightning rods of different geometries were carried out near the 3288-m-high summit of South Baldy Peak, New Mexico [8], [9]. It was found that after seven years of tests, none of the sharp Franklin rods or of the so-called Early Streamer Emitters have been struck by lightning. Most of the strikes have been to 19 mm diameter rods with hemispherical tips, while none of the 9.5 mm diameter and 51 mm diameter rods were hit. So far, these field test results have not been satisfactorily explained. Nevertheless, the clear advantage reported for blunt rods led to their acceptance as an alternative to sharp rods by the NFPA [10].

As will be shown, the failure of the sharp rods to be struck by lightning in the New Mexico tests is a clear demonstration of space charge shielding which may impact their ability to offer effective protection to a nearby object, such as a building corner [11].

This paper has been written with the following objectives.

1) Model the response of a lightning rod to both the slowly varying ambient electric fields due to cloud charges prior to negative leader descent and the impulse-type field generated by a descending negative leader.
2) Specifically investigate the effect of the lightning rod shape on both streamer onset and the inception of an upward positive leader.
3) Include in the analysis not only geometrical parameters, such as rod diameter and height, but also surface protrusions and air density.
4) Distinguish lightning rods in terms of discharge response rather than simple geometrical shape.
5) Model the effect of corona space charge at the lightning rod tip prior to negative leader descent, not only for rods on flat ground but for a rod installed at the top of a massive structure.

Manuscript received December 14, 2009; revised March 27, 2010 and April 21, 2010. First published September 07, 2010; current version published September 22, 2010 Paper no. TPWRD-00926-2009.

The author is with Expodev, Inc. and Lightning Electrotechnologies, Inc., Montreal, QC J4S 1W2, Canada.

Color versions of one or more of the figures in this paper are available online at http://ieeexplore.ieee.org.

Digital Object Identifier 10.1109/TPWRD.2010.2049384

II. Streamer Corona Onset

It is well known that when the electric field on the surface of an electrode reaches a critical value, corona discharge is initiated [12]. The corona onset gradient depends on the electrode geometry, surface conditions, as well as on the ambient atmospheric conditions. There is more than one century of experience with the corona discharge [12] and these days, corona onset conditions can be reliably accounted for analytically [13]. An excellent experimental investigation of corona modes from hemispherical and conical protrusions is described in [14]. For a positive point in steady or slowly varying electric fields, these modes include onset streamers, glow, a mixture of streamers and glow and, for air gaps, breakdown streamers [14].

In the following sections, positive streamer corona onset conditions from the tip of a grounded lightning rod are analyzed. This aspect is fundamental since a critical streamer from a rod comprises a prerequisite for positive leader formation [15]–[17].

A. Field Intensification

In the following sections, the terms ground field and ambient field are used. Ground field is the electric field at ground level. Ambient field is, in general, the electric field in which a mast or a lightning rod is immersed. If assumed uniform, the ambient field would be identical to the ground field.

If a grounded lightning rod is immersed in a uniform ambient electric field $\mathrm{E_g}$, rod slenderness leads to a substantial intensification of the field $\mathrm{E_t}$ at the tip of the rod. This field intensification can be calculated analytically only by assuming simple rod shapes, such as a semi-ellipsoid [8]. For hemispherically capped and sharp rods, this can be accurately accomplished by numerical methods, such as the charge simulation technique [18]. Fig. 1 shows the resulting field intensification factor $\mathrm{f} = \mathrm{E_t}/\mathrm{E_g}$ for a hemispherically capped rod of height h and radius r as function of the slenderness ratio h/r in the range 80–3200. For example, at $\mathrm{h/r} = 80$, the field intensification factor is 62.5, while for $\mathrm{h/r} = 400$, it reaches 260. For comparison, with a semi-ellipsoidal rod with height h and radius of curvature r at the tip, the field intensification factors for $\mathrm{h/r} = 80$ and 400 as before become only 41.6 and 148.2, respectively.

B. Onset Gradient

The corona onset gradient $\mathrm{E_{ci}}$ from a smooth rod tip depends on the tip radius of curvature r and the relative air density δ, and can be calculated [17], based on the streamer theory by the expression

$$\mathrm{E_{ci}} = 2300 \cdot \delta \left[1 + \frac{0.224}{(\delta \mathrm{r})^{0.37}}\right]. \quad (\mathrm{kV/m, m}). \qquad (1)$$

For electrode surfaces with protrusions, water drops, etc., a surface roughness factor $\mathrm{m} < 1$ [13] can be introduced in the above expression

$$\mathrm{E_{ci}} = 2300\,\mathrm{m} \cdot \delta \left[1 + \frac{0.224}{(\delta \mathrm{r})^{0.37}}\right]. \quad (\mathrm{kV/m, m}). \qquad (2)$$

The roughness factor m is normally determined by comparing the experimental onset gradients of smooth and rough conductors. On cylindrical transmission line conductors, the presence of water drops could result in m values in the range 0.3–0.6, while a thick uneven layer of soil may reduce m to 0.2 or lower [13].

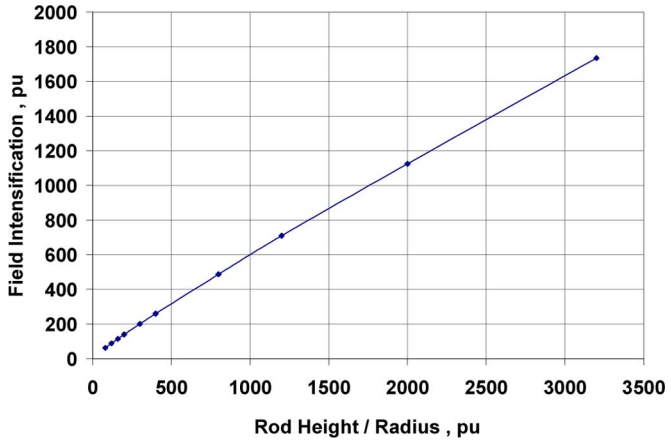

Fig. 1. Variation of the field intensification factor on the rod height to radius ratio. Hemispherically capped rod in the uniform field.

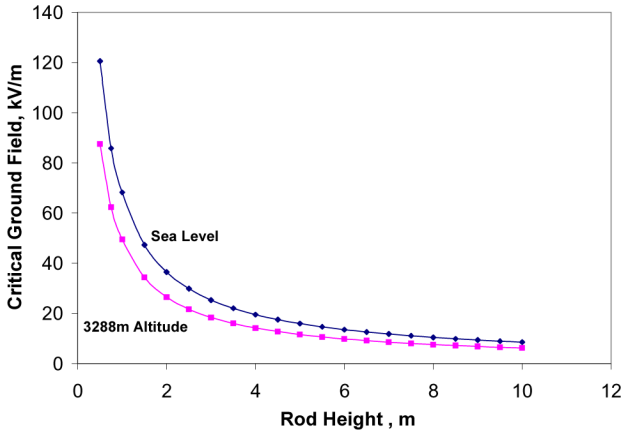

Fig. 2. Variation of the critical ground field for corona inception $\mathrm{E_{gci}}$ with a height of 2-cm diameter rod at different altitudes.

While surface roughness due to the water drop leads to substantial reduction in the corona onset gradient and positive switching impulse breakdown voltage of large-electrode gaps as mentioned before, rain tests with sharp rods showed no difference from dry tests [7]. Furthermore, it is clear that the larger the exposed electrode surface area is, the more susceptible it is to being contaminated by water drops, insects, etc. under realistic field conditions.

If the field intensification factor f of a lightning rod of given dimensions is determined by using (1) or (2), it allows one to establish the value of the critical ground field for corona onset $\mathrm{E_{gci}}$. Fig. 2 shows variations of the critical ground field for corona inception with a height for a rod with 2 cm diameter, at sea level and at an altitude of 3288 m ($\delta = 0.667$ [19]). As expected, the critical ground field will be lower at higher altitude.

As shown in [20], the ground field due to cloud charges is a statistical variable whose distribution appears to vary from one region to another.

Statistical distribution of ground fields due to cloud charges is normally truncated upwards with a maximum value $\mathrm{E_{gm}}$ [20].

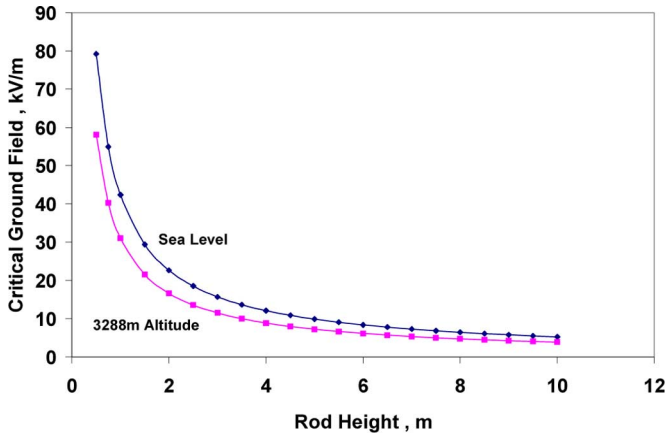

Fig. 3. Variation of the critical ground field for corona inception $\mathrm{E_{gci}}$ with height for a 1 cm diameter rod at different altitudes.

Fig. 2 shows that for $\mathrm{m} = 1$, a 2 cm diameter, 8.5 m rod would not go into corona prior to the descent of a downward stepped leader if the maximum ground field $\mathrm{E_{gm}}$ is limited to 10 kV/m. For a relative air density of 0.667 (altitude 3288 m) on the other hand, with the same $\mathrm{E_{gm}} = 10$ kV/m, the maximum height of a 2-cm rod that does not go into corona prior to stepped leader descent becomes only 6 m. The significance of these results will be made clearer. Since the ground field due to cloud charges does not normally exceed 20 kV/m, it may be tempting to believe, based on Fig. 2, that short rods below 1 m length, as normally recommended by NFPA [10], would not go into corona prior to negative stepped leader descent. This is, however, unjustified since these rods are installed at rooftops of buildings where they are immersed in fields that are much higher than the fields at ground level [11].

Fig. 3 shows similar results, with $\mathrm{m} = 1$, but for a lightning rod of 1 cm diameter. As would be expected for the same rod height, the critical ground field for corona inception is significantly lower for the 1 cm than for the 2 cm rod. Here, at sea level and with $\mathrm{E_{gm}} = 10$ kV/m, the maximum rod height with out corona due to the cloud charge field is 5 m at sea level and only 3.5 m at a relative air density of 0.667. At this reduced air density, a 6.5-m-high, 1-cm-diameter rod would go into corona at $\mathrm{E_g} = 5.7$ kV/m.

III. Leader Inception

Research on long air gaps by Les Renardières Group [4] has confirmed that except for electrodes with radii above the so-called critical radius [16] corresponding to the electrode height above ground concerned, streamer onset is a necessary but insufficient condition for continuous leader formation. Contrary to corona onset which is primarily determined by the electric field and field gradient at the electrode surface, leader inception depends on electric field distribution in a considerable volume to be occupied by streamers in the electrode vicinity. In [15], the conditions for continuous leader inception were formulated in terms of:

- a critical streamer size which is responsible for the formation of a highly ionized stem at its root;
- maintaining a critical electric field at the leader tip during its propagation; this electric field comprises two major components: 1) an applied electric field and 2) an opposing component due to the streamer space charge or so-called leader corona.

This model was adapted to apply for upward leader formation from grounded objects [21]. It was applied to assess lightning exposure of high voltage transmission lines [21] and has been recommended in [22]; however, occasionally the following questions have been raised.

- Why would a leader inception criterion originally developed for high voltage electrode-ground gaps be applied to upward leader formation from a grounded object?
- Why would a model originally formulated for the switching impulse voltages of a double-exponential form and their associated fields apply to lightning when the time variation of ground fields obviously do not follow a double exponential pattern?

Let us first establish that all models addressing upward leader inception from ground structures [23]–[26] have their origins in laboratory gaps, so the aforementioned questions apply to all of those models.

The answer to the first question is quite basic. Ionization by electron collision in the stressed volume around the structure tip depends on the electric field distribution in that zone. Under the same electric field magnitude and distribution, electrons would not "feel" the difference between an energized or a grounded structure. The essential point then is to determine the conditions under which the field distribution in the stressed volume in the vicinity of the tip would be practically the same for two situations. The first is a rod-plane gap with the rod maintained at a distance h above ground and energized at a voltage U. The second is a grounded rod of height h immersed in a uniform ambient field $\mathrm{E_g}$. The necessary and sufficient condition is

$$U = E_g \cdot h. \tag{3}$$

A demonstration of this is shown in Fig. 4, where the electric field distribution below the rod tip along the axis of a 30 m rod-plane gap, with a rod of 10 cm diameter, energized at $\mathrm{U} = 1000$ kV is compared with the axial electric field distribution above the tip of a grounded mast of the same diameter with height $\mathrm{h} = 30$ m, immersed in a uniform ambient field $\mathrm{E_g} = 33.33$ kV/m. These parameters satisfy (3) above and it is clearly shown that the two field distributions are very close.

For the grounded rod of height h, immersed in a uniform ambient field $\mathrm{E_g}$, the quantity

$$U_{\mathrm{sp}} = E_g \cdot h \tag{3a}$$

is called the space potential. In a nonuniform ambient field, $\mathrm{E_g}$ is replaced by the mean value along a height h.

From the aforementioned analogy between an energized rod at voltage U in an air gap h and a grounded rod of height h immersed in an ambient field, $\mathrm{E_g}$ will be valid if the space potential $\mathrm{U_{sp}} = \mathrm{U}$ or if the ambient field in the lightning case satisfies $\mathrm{E_g} = \mathrm{U/h}$.

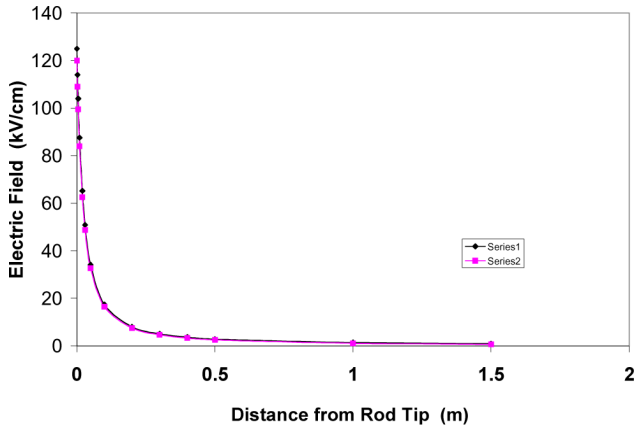

Fig. 4. Variation of the axial electric field with distance from the tip of the hemispherically capped 10 cm diameter rod. S1:30 m lightning mast on ground plane, $\mathrm{E_g} = 33.33$ kV/m. S2: 30 m rod-plane gap, $\mathrm{U} = 1000$ kV.

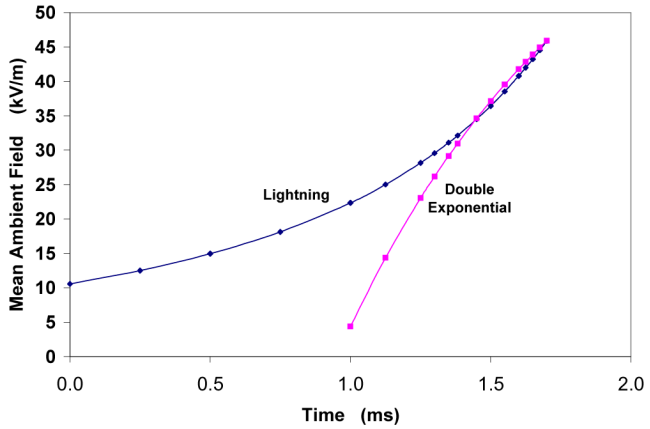

Fig. 5. Variation of mean ambient field in which a 30 m mast is immersed with time during negative leader descent and comparison with double exponential impulse of 3.6 ms front. Initial leader height: 500 m, radial distance: 89 m. $\mathrm{I} = 31$ kA, leader speed: 2×10^5 m/s.

During negative leader descent, the ambient field in which a grounded structure is immersed rises with time. The field variation at any instant depends on the leader charge, which, in turn, is related to the prospective return stroke current I [24], the leader height above the structure tip, and its radial distance from it as well as on leader speed.

Fig. 5 shows the variation with time of the mean ambient field in which a 30 m grounded mast is immersed during descent of a negative leader with prospective return stroke current $\mathrm{I} = 31$ kA, a radial distance of 89 m, corresponding to the maximum attractive radius of the mast for the parameters involved [21]. The negative leader speed is taken as 2×10^5 m/s and the origin of the time scale corresponds to the instant when the leader tip was 500 m above ground. The calculation stops when the mean ambient field reaches 46 kV/m which, according to [21], corresponds to inception of a continuous upward connecting leader from the 30-m rod tip. It is shown that the ambient field rises slowly first, with the rate of rise increasing with time as it approaches the positive upward leader inception level.

Fig. 5 also shows the field variation with time following a double-exponential function, selected to coincide with the mean ambient field values due to the descending leader at the upward leader inception level of 46 kV/m and at 70% of that value (32 kV/m). It is shown that here for a front time $\mathrm{t_f} = 3.6$ ms field variations for both lightning and the double exponential curve are quite close in the upper 30% of the field range. It is clear, however, that at lower field levels, the discrepancy between the two curves is substantial. Laboratory experience with long air gaps under positive switching impulse voltages however has demonstrated that:

- the lower part of the impulse has no significant effect on leader inception or breakdown [27]; this follows from comparative tests with double exponential impulses obtained from an impulse generator and a 1-cosine form generated by switching an HV test transformer [28];
- the longer the air gap is, the less sensitive the critical breakdown characteristics are to the impulse front [28] so that the value of $\mathrm{t_f}$ used to fit the upper part of the field curve is not critical;
- based on similar arguments, it has been previously shown [29] that for shorter lightning rods, double exponential impulses with front times in the range 200 μs–1 ms are suitable to simulate upward leader inception; subsequently, double exponential impulses of 250 μs and 580 μs fronts were used for lightning simulation tests on 0.5 m and 1.0 m lightning rods [29].

Consider a lightning rod of radius r and height h over flat ground in an ambient relative air density δ. If the rod is exposed to a slow front ambient field as typically produced by a negative stepped leader, ignoring for the moment space charge effects due to cloud charge fields, it can been shown [30] that the critical mean ambient field for continuous upward leader inception can be expressed by

$$E_{\mathrm{gc0}} = \frac{1556}{h + \frac{3.89}{\delta}} \quad (\mathrm{kV/m, m}). \tag{4}$$

This corresponds to a critical leader inception space potential $\mathrm{U_{spc0}}$ given by

$$U_{\mathrm{spc0}} = \mathrm{E_{gc0}} \cdot h = \frac{1556}{1 + \frac{3.89}{\delta \cdot h}} \quad (\mathrm{kV, m}). \tag{5}$$

The radius of a grounded rod for which the mean ambient field, or space potential for corona inception and for continuous leader inception coincide, is called the critical radius for the height concerned [16]. In other words, for such a rod, corona inception would immediately lead to continuous positive upward leader formation. For tall structures prone to upward flashes, however, conditions for continuous upward leader inception are formulated in [20]. It has been shown previously that for rods with radii below the critical radius, the critical ambient field, or space potential, for continuous leader inception is independent of the radius of the rod [16], [21].

Using charge simulation [18] to determine the corona inception mean ambient field $\mathrm{E_{gci}}$ for different rod radii, the critical radius is determined, at which for a given rod height h, $\mathrm{E_{gci}}$ is equal to the continuous leader inception mean ambient field $\mathrm{E_{gc0}}$ from (4). The results are shown in Fig. 6 for $\delta = 1$ (sea level) and for $\delta = 0.667$ (3288 m altitude). It is shown that at any rod height, the critical radius is increased at high altitude.

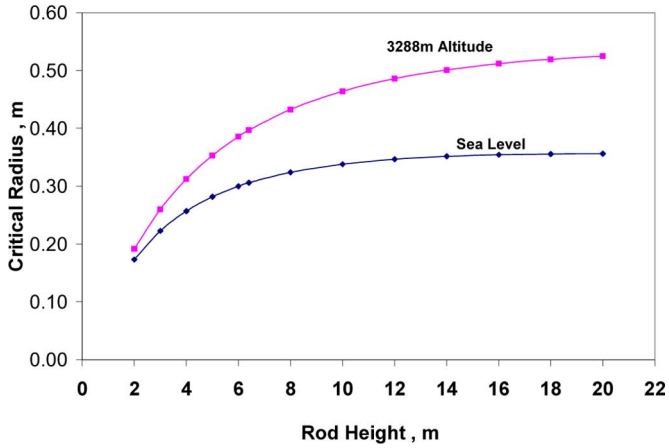

Fig. 6. Variation of the critical radius for upward leader inception of a hemispherically capped rod with rod height above ground at different altitudes.

A similar result is found in [31]. It is also shown that the critical radius first increases but ultimately saturates at larger rod heights. Finally it is found that through the whole range of rod heights $2 \leq \mathrm{h} \leq 20$ m, that the critical radius is far above any radius of a practical lightning rod.

It follows that under these conditions, the variation of the diameter of a lightning rod in the range of 9.5 to 51 mm [8], [9] should practically have no effect on the lightning exposure of these rods. This conclusion is supported by outdoor laboratory experience [32], which established that there was no difference in the experimental striking frequency between sharp and blunt rods, contradicting the field test results of Moore *et al.* [8], [9]. The same conclusion was reached based on modeling work in [33]. However, [34] reported on a slightly optimum dimension found from model results for a 10 m rod, of practically the same diameter of 19 mm as the rod struck most in the field experiments of Moore *et al.* [8], [9]. This was apparently achieved without consideration to the effects of rod height, relative air density, or the intensity of the ambient field due to cloud charges prior to negative leader descent.

In the following section, an explanation of the aforementioned controversy will be sought by exploring the effects of corona space charge due to the ambient ground field prior to the descent of the negative leader.

IV. Space Charge Due to Cloud Charges Prior to Leader Descent: Effect on Upward Leader Inception

There is ample theoretical [35], [36] and experimental [37]–[39] evidence that the presence of positive dc corona space charge in the vicinity of a highly stressed electrode prior to the application of positive impulse-type stress tends to inhibit positive leader formation. It has been shown in [35] that for a grounded sphere (point electrode) high above ground, exposed to an ambient field due to cloud charges, corona formation substantially reduces the electric field in the tip vicinity below the values needed for critical streamer formation. As mentioned previously, the formation of these streamers is a prerequisite for continuous upward leader inception. It is important to note that here we are dealing with ambient fields due to cloud charges with durations of several seconds, which produce considerable charge in a relatively large volume. This is in contrast to the lower part of the impulse component which has a duration in the range of hundreds of microseconds to a few milliseconds and which was shown above to have little effect on leader inception. A stress comprising a dc field, space potential, or voltage in the case of air gaps, followed by an impulse-like component is called a composite stress [39]. Laboratory test results on long air gaps under positive composite dc and switching impulse voltages have been reported in [37]–[39]. It was shown that if the dc component is below the corona inception level of the highly stressed electrode, this component will have practically no effect on leader inception or breakdown of the air gap. If, on the other hand, the dc component is above corona inception level, the positive corona space charge leads to an increase in the leader inception level and accordingly the air gap breakdown voltage. This phenomenon has been proven beyond any doubt and has important practical consequences on the performance of air insulation of HVDC transmission lines [39], [40].

In this section, an analytical approach is used to quantify the effect of corona space charge due to the dc field caused by cloud charges, prior to negative leader descent, on upward leader inception. A simplified and idealized but instructive configuration is that of a small grounded sphere of radius $\mathrm{r_o}$ at a height h above ground immersed in an ambient ground field which increased gradually to reach a value $\mathrm{E_{g0}}$ [35].

Assume that $\mathrm{E_{g0}}$ is greater than the corona inception ground field $\mathrm{E_{gci}}$ of the grounded electrode. It is generally assumed that during the growth of the corona space charge zone, the electric field on the electrode surface is maintained at the corona inception field $\mathrm{E_{ci}}$ [13], [35]. It follows that the charge $\mathrm{Q_i}$ induced by corona space charge on the spherical electrode is given by

$$Q_i = -4\pi \in_0 r_0^2(E - E_{\mathrm{ci}}), \tag{6}$$

where E is the electric field that would have existed on the grounded sphere in the absence of the space charge

$$E = E_{g0} \cdot h/r_0 \tag{7}$$

since for a free sphere, the field intensification factor $\mathrm{f} = \mathrm{h}/\mathrm{r_0}$.

Substituting in (6)

$$Q_i = -4\pi \in_0 r_0(E_{g0} \cdot h - r_0 E_{\mathrm{ci}}). \tag{8}$$

Substituting for $E_{g0} \cdot h = V_0, r_0 E_{\mathrm{ci}} = V_{\mathrm{ci}}$, where $\mathrm{V_0}$ and $\mathrm{V_{ci}}$ are called the dc space potential due to cloud charges and the corona inception space potential of the sphere, respectively

$$Q_i = -4\pi \in_0 r_0(V_0 - V_{\mathrm{ci}}). \tag{9}$$

Since $-Q_i/4\pi \in_0 r_0$ is the space potential induced by the corona space charge, $\mathrm{U_{sc}}$, it follows that:

$$U_{\mathrm{sc}} = V_0 - V_{\mathrm{ci}}. \tag{10}$$

Expression (10) was checked by the numerical solution of the corona space charge equations according to [35]. A grounded solitary sphere of radius 5 cm as considered in [35] was placed at a height of $\mathrm{h} = 150$ m and immersed in a uniform ambient field due to cloud charges that increased linearly to reach $\mathrm{E_{g0}} = 10$ kV/m in 10 s. From (1), the corona onset field $\mathrm{E_{ci}}$ amounts to

38.6 kV/cm so that the corona onset space potential $V_{ci} = 193$ kV. The dc space potential $V_0 = E_{g0} \cdot h = 1500$ kV. According to (10), the corona space charge induced potential $U_{sc} = 1307$ kV. The numerical solution following [35] yielded a maximum corona current of 228.5 μA and a corona charge of 1.524 mC. This corona space charge cloud resulted in an induced potential $U_{sc} = 1299.6$ kV. The agreement with (10) is excellent.

Let the critical upward leader space potential in the presence of such corona space charge be U_{lc} and in its absence U_{lc0}, it follows that:

$$U_{lc} - U_{sc} = U_{lc0}. \tag{11}$$

Substituting from (10)

$$U_{lc} = U_{lc0} + (V_0 - V_{ci}). \tag{12}$$

In terms of the critical leader inception mean, ambient fields E_{gc} and E_{gc0}, in the presence and in the absence of space charges due to cloud charge fields, respectively, divide (12) by the height h

$$E_{gc} = E_{gc0} + \left[E_{g0} - \frac{r_0 E_{ci}}{h}\right] \tag{13}$$

where E_{g0} is the ground field due to cloud charges.

The quantity $r_0 E_{ci}/h$ is the corona inception ground field E_{gci} so that (12) becomes

$$E_{gc} = E_{gc0}\left[1 + \frac{(E_{g0} - E_{gci})}{E_{gc0}}\right] \tag{14}$$

which applies for $E_{g0} > E_{gci}$ whereas for $E_{g0} \leq E_{gci}, E_{gc} = E_{gc0}$.

Equation (14) shows that E_{gc}/E_{gc0} increases linearly with the ratio $(E_{g0} - E_{gci})/E_{gc0}$. This means that this amplification factor will increase with higher static or slowly varying fields E_{g0} due to cloud charges, at lower corona inception ground field (e.g., smaller radius r_0 and with larger height h), which from (4) reduces E_{gc0}.

The solution of Poisson's and the continuity equation was undertaken for a concentric sphere-grounded sphere configuration, with the applied voltage V_0 exceeding the corona inception voltage V_{ci}. It was found that for the same V_0 and V_{ci} as above and for the same size of the space charge zone, the corona charge in the concentric sphere configuration exceeded the corresponding charge in the free grounded sphere case by a factor of 3/2. However, when the effect of image charges on the grounded sphere is taken into consideration, as it must, the space charge induced potential U_{sc} was found to be identical to (10).

It may therefore be concluded that for a grounded electrode immersed in an ambient field and for a laboratory gap, when the space charge symmetrically surrounds the electrode in corona, (10) fully applies. However, since the space charge pattern will, in general, be influenced by the electrode shape and height above ground, (10) will be used for a lightning rod as a first estimate of the space charge induced potential.

If the field intensification factor at the rod tip is designated by f, then E_{gci} in (14) could be replaced by

$$E_{gci} = E_{ci}/f \tag{15}$$

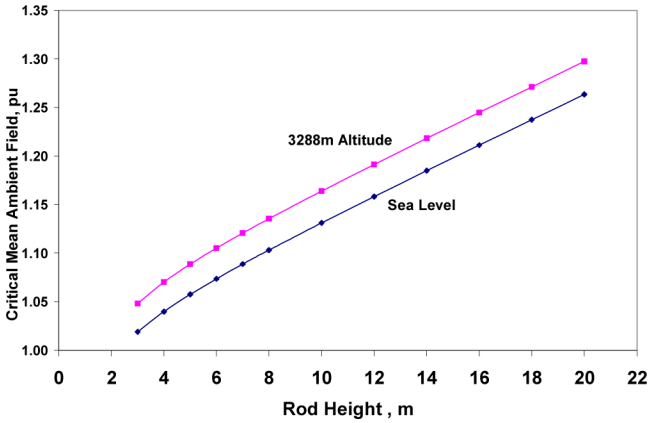

Fig. 7. Variation E_{gc}/E_{gc0} due to the corona space charge with a height of a 1 cm-diameter hemispherically capped lightning rod. $E_{gm} = 20$ kV/m, at different altitudes.

where E_{ci} is the corona inception field at the rod tip, expressed by (2).

It follows from the above that if two adjacent lightning rods are simultaneously exposed to the same ambient conditions, the rod that does not go into corona under the maximum ambient ground field due to cloud charges, prior to negative leader descent, will be the one most likely to produce a continuous upward connecting leader. It will therefore be the one most likely to be struck by lightning. On the other hand, the rod with low corona onset ambient ground field E_{gci} will have a tendency due to space charge shielding to self-protect.

Fig. 7 shows the variation of the ratio E_{gc}/E_{gc0} between the continuous leader inception ambient field of a 1-cm-diameter hemispherically capped rod in the presence of the corona space charge at the rod tip, to the corresponding value for a rod that is corona free prior to negative leader descent, as a function of the rod height h above ground, as determined from (14). E_{gci} was determined from (15) with f of the lightning rod calculated by charge simulation.

The results are presented for seal level and for a 3288 m altitude. Here, the maximum ground field due to cloud charges is taken as 20 kV/m ($E_{g0} = E_{gm}$). If a maximum ground field due to cloud charges is taken as 5 kV/m instead, the effect of corona space charge due to the cloud charge field will be negligible.

As previously mentioned, the effect of corona due to the cloud charge field in the vicinity of a sharp rod tip on upward leader inception is not restricted to tall rods. A rod installed on a tall structure is of practical interest.

In the following text, the term dc-corona will refer to corona due to the cloud charge field prior to the descent of the negative leader.

The above approach was applied to a 2 m, 1 cm-diameter rod installed at the center top of a 180 m cylindrical mast with 4 m diameter. The ground field E_{g0} due to cloud charges was assumed to be 5 kV/m. By charge simulation, the corona inception ground field E_{gci} of the rod was determined at only 0.76 kV/m. Again, using charge simulation, with due consideration to the massive mast proximity effect [11], the corresponding value E_{gc0} is determined at 9.84 kV/m. The upper limit of E_{gc} is in per unit of the corresponding value E_{gc0} of a dc-corona

free rod as determined from (14), amounting to 1.43, indicating substantial space charge shielding due to corona produced cloud charge fields, despite the limited height of the rod.

A comparison has been made between a dc-corona-free rod of 2 m length and a 4 m sharp rod which, of course, is prone to dc-corona formation, when placed atop the 180 m mast as described before. It was found that the leader inception ground field $\mathrm{E_{gc0}}$ of the dc-corona free rod is 9.84 kV/m as mentioned before. The corresponding value $\mathrm{E_{gc}}$ for the 4 m sharp rod amounted to 15.1 kV/m, confirming the advantage of a dc-corona-free rod even though it was shorter. Evidently, however, if we keep increasing the length of the sharp rod, a length would be reached where the leader inception ground field of the tall rod becomes lower than the corresponding value of the 2 m dc-corona free rod considered before. This tall rod, however, becomes more vulnerable to space charge effects, and due to the statistical variability of ground fields due to cloud charges, the protective characteristics of the rod become less predictable as demonstrated by field experience where tall masts are sometimes struck on the side below the top [1]. As well, these tall rod heights may be less practical.

V. Space Charge due to Cloud Charges Prior to Leader Descent: Effect on Attractive Radius

As shown in (14), the space charge created in the vicinity of a lightning rod tip, due to cloud charge field prior to leader descent, leads to an increase in the continuous upward leader inception ambient ground field expressed by the ratio $\mathrm{E_{gc}/E_{gc0}}$ which expresses the leader inception ambient field in per unit, with a base of $\mathrm{E_{gc0}}$.

It should be noted that the positive ion space charge created due to a cloud charge field in a typically 10 s duration, does not move significantly during the negative leader descent of a few milliseconds duration. Consider a negative leader descending at a radial distance from an air terminal in-corona corresponding to the attractive radius of a corona-free air terminal. This defines the boundary of the area within which a descending leader, with a given prospective return stroke current, would be collected by a corona-free air terminal. During any delay in upward leader initiation due to the space charge, the downward leader will continue its downward movement. This will reduce the time available for the upward leader, from the air terminal in-corona, to complete its trajectory into a successful encounter by streamer breakdown between the two leader tips. The downward leader will then either strike another object or strike the ground.

To counteract the effect of such a delay, the downward leader has to be radially closer to the air terminal in corona to ensure a successful encounter. By definition, this means a shorter attractive radius. Delaying upward leader inception due to space charge will therefore have a definite impact on the attractive radius as explained before. The degree of this impact will depend on the height of the rod and the magnitude of the ambient field due to cloud charges.

The distinction between the terms, attractive radius, and striking distance has been addressed in [21].

An instructive example for the decrease of the attractive radius (distance) of an air terminal due to an increase in the critical ambient field for continuous upward leader initiation follows from the comparison of lightning exposure of ground wires and slender masts. It is well known that a ground wire has a higher critical ambient field for continuous upward leader onset than a slender mast of the same height [21]. It is also known that this ground wire has a smaller lateral attractive distance $\mathrm{D_a}$ than the attractive radius $\mathrm{R_a}$ of the mast [21]. As a numerical example, the critical ambient field of a 20-m-high, 2-cm diameter ground wire amounts to 94.9 kV/m, while the corresponding value for a 20 m mast is 65.1 kV/m [21]. It has been found that the ratio $\mathrm{D_a/R_a}$ varies from 0.72 for a return stroke current of 3 kA to 0.79 at 15 kA (i.e., a 46% increase in the critical ambient field resulting in a 21%–28% reduction in the attractive radius (distance)). In [41], Eriksson assumed this ratio to be 0.8, independent of the return stroke current. Whether the increase in the critical ambient field for continuous upward connecting leader initiation is achieved by geometrical or space charge effects, the resulting trend of a reduced attractive radius should be no different.

In the following sections, the term corona free refers to rod performance under the effect of the maximum field due to negative cloud charges prior to the negative leader descent.

Applying the model described in [21], Fig. 8 shows the reduction of the attractive radius $\mathrm{R_a}$ since the leader inception ambient ground field increased in the range 1.0–1.18 p.u., of a 10 m rod for prospective return stroke currents I of 10 and 30 kA. It is shown that for $\mathrm{I} = 30$ kA, an 18% increase in the leader inception ambient field due to space charge, formed before negative leader descent, leads to a reduction in the attractive radius $\mathrm{R_a}$ from 69.7 m to 64.2 m, an 8% reduction. This corresponds to a reduction of the attractive area which determines exposure to lightning by approximately 15%. We can therefore conclude that for this rod height, space charges at the tip of a solitary rod due to ambient ground field before negative leader descent will have a limited effect on rod exposure to lightning. On the other hand, this increase in the continuous upward leader inception ambient field will have a determining effect on settling the race between a sharp and blunt rod of practically the same height. Or more generally between objects in corona and dc-corona-free objects subjected to the same ambient conditions, as was the case in the field experiments reported in [8] and [9].

VI. Non-Self Shielding Air Terminal

The aforementioned analysis leads to a general physical definition of a non-self shielding air terminal. This air terminal does not simply become a rod of fixed diameter with a hemispherical top but should rather satisfy certain performance criteria which can be formulated as follows.

- The air terminal must not go into corona below the maximum ambient ground field due to cloud charges prior to negative leader descent.
- The dry corona inception ambient field of the air terminal must not exceed the critical leader inception ambient field (i.e., the equivalent radius of the air terminal must not exceed the critical radius for the height involved).
- The air terminal must not have such a large diameter as to be impractical or to become too susceptible to water drops, protrusions, etc., leading to deteriorated corona performance, effectively approaching that of a sharp rod (i.e.,

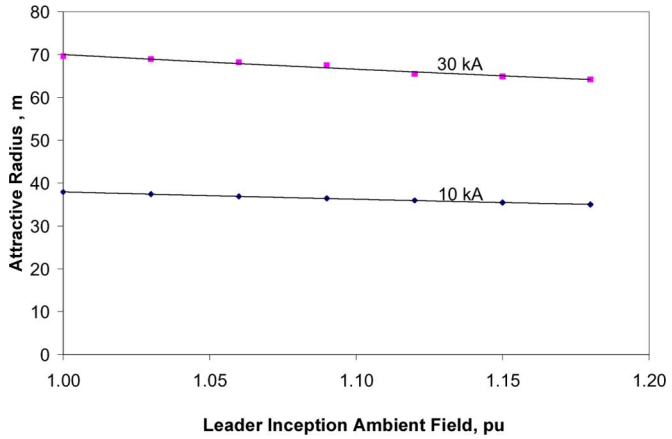

Fig. 8. Attractive radius of a 10 m rod to a negative descending leader: Effect of the relative increase in the critical upward leader inception field, caused by the space charge in the vicinity of the rod tip due to the cloud charge field ($\mathrm{E_{gm}}$ = 20 kV/m) prior to the negative leader descent.

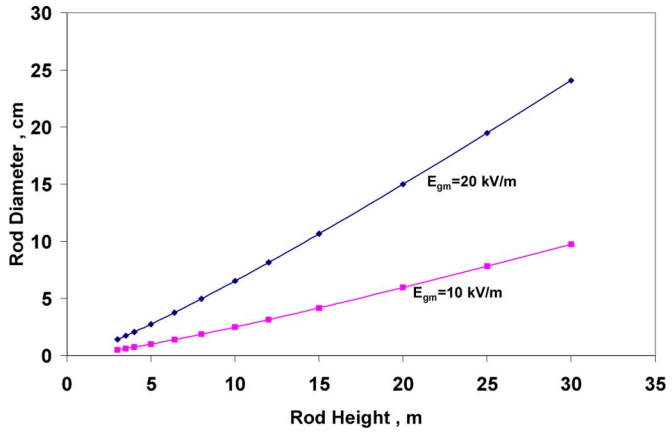

Fig. 9. Variation of the dc-corona free Franklin rod diameter with the tip height above ground for two levels of the maximum ground field due to cloud charges.

the smaller radius of the rod, which satisfies the above conditions, the better).

As will be shown, in some cases, a simple hemispherically capped rod would satisfy the aforementioned requirements, but this is by no means always the case.

Fig. 9 shows the variation of the diameter of a hemispherically capped rod whose corona inception ground field $\mathrm{E_{gci}}$ coincides with the maximum ground field due to cloud charges, for $\mathrm{E_{gm}}$ of 10 kV/m and 20 kV/m. It is clearly shown that the required rod diameter to avoid space charge shielding, due to cloud charge fields, varies considerably with the rod height and is moreover sensitive to the maximum ground field in the region concerned. In the results of Fig. 9, which are determined at sea level ($\delta = 1$), the ratio between the rod height h and the required radius r is not constant but also varies with height h and with the maximum ambient ground field $\mathrm{E_{gm}}$. For $\mathrm{E_{gm}}$ of 20 kV/m, h/r drops from 422 at $\mathrm{h} = 3$ m to 249 at $\mathrm{h} = 30$ m. For $\mathrm{E_{gm}}$ of 10 kV/m, on the other hand, h/r drops from 1188 at $\mathrm{h} = 3$ m to 616 at $\mathrm{h} = 30$ m. Similar results are shown in Fig. 10 for $\mathrm{E_{gm}} = 10$ kV/m, where the variation of the dc-corona-free rod diameter is shown as a function of the rod height for two altitudes: 1) at sea level and 2) at an altitude of 3288 m ($\delta = 0.667$). It is

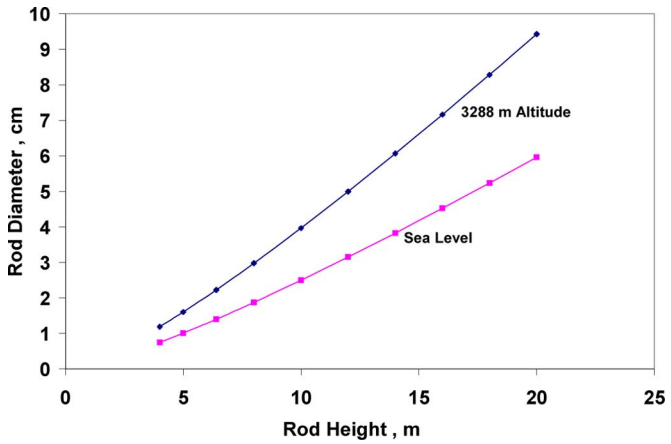

Fig. 10. Dependence of the required rod diameter for the dc-corona free performance on the rod height at different altitudes. Maximum ground field: 10 kV/m.

clear that for a fixed rod height, the diameter of the required dc-corona-free rod increases significantly at higher altitude. The ratio h/r also varies with the relative air density. For $\mathrm{E_{gm}}$ of 10 kV/m, as before, h/r drops from 745 at $\mathrm{h} = 3$ m to 424 at $\mathrm{h} = 20$ m. Specifically, for $\mathrm{h} = 6.4$ m, $\mathrm{h/r} = 575$, which is not far from the apparent optimum ratio of approximately 680 obtained from the New Mexico experiments [8], [9]. More about those tests will be given.

The results of Figs. 9 and 10 also show that at larger rod heights, the required diameter for a dc-corona-free lightning rod under the maximum ground field due to cloud charges becomes impractically large and susceptible to deteriorated corona performance due to protrusions and water drops.

VII. Comparison with Experiment

In this section, the model findings will be compared with field test results on different sharp and blunt rods described in [8] and [9].

A. Corona Performance of Lightning Rods

The charge simulation technique [18] was used to perform electric field calculations on lightning rods immersed in a uniform ambient field, for the configurations described in [8] and [9]. The mast supporting the lightning rods had a height of 6.1 m and a diameter of 44 mm. Lightning rods of 30 cm length were installed on top of the mast resulting in a tip height above ground of 6.4 m. The rod geometries simulated included a sharp rod with a 0.1 mm tip radius as well as hemispherically capped rods with diameters 9.5 mm, 12.7 mm, 19 mm, 25.4 mm, and 51 mm [8], [9]. The sharp rod was simulated in great detail and consisted of a right cylinder part, a tapered part, a conical part, and finally the tip. For each rod, the corona inception field $\mathrm{E_{ci}}$ at the 3288 m altitude was determined. The field intensification factor was also calculated, from which the corona inception ground field $\mathrm{E_{gci}}$ was found. This was compared to the measured values when available and to an assumed maximum field value of $\mathrm{E_{gm}} = 10$ kV/m [8].

Table I contains charge simulation results on the corona inception characteristics of the various rods. For blunt rods, the corona inception ground field was found to exceed 5 kV/m in

TABLE I
CORONA INCEPTION CHARACTERISTICS OF DIFFERENT RODS AT 3288 m ALTITUDE

ROD TYPE	E_{ci}, kV/cm	E_{gci}, kV/m
Sharp (tip radius 0.1mm)	135.9	0.80
9.5mm diameter	44.2	5.93
12.7mm diameter	41.3	7.18
19mm diameter	37.8	9.36
25.4mm diameter	35.4	11.27
51mm diameter	30.9	17.80

TABLE II
LIGHTNING EXPOSURE OF COMPETING RODS (1994–1997) [8]

	Number of Strikes	
Rod Type	Natural	Triggered
Sharp (0.1mm tip)	0	0
9.5mm diameter	0	0
12.7mm diameter	1	2
19.0mm diameter	2	3
25.4mm diameter	1	0
51mm diameter	0	0

good agreement with the experiment [8]. For the sharp rod, on the other hand, the corona inception ground field with a tip of 0.1 mm radius amounts to 0.8 kV/m, while the reported field value is 2.0 kV/m. (Private communication with one of the authors of [8] indicated a value of 1 kV/m.)

The ground fields in Table I and in the reported measurements refer to values in the vicinity of the lightning rods at the test site. Accordingly and due to the obvious fact that the rod height is extremely small compared to the mountain dimensions, mountain topology will have no effect on the comparison between theory and field measurements reported before. Furthermore, any ground field nonuniformity effect due to point discharges in the environment (grass, bushes, etc.) was considered following the approach of Wilson [42]. A conservative situation discussed in [43] was analyzed, in which the corona onset ground field from bushes was 3 kV/m, the ground field $\mathrm{E_{g0}}$ considered was 8 kV/m, and the corresponding corona current density $\mathrm{J_c}$ amounted to 1 nA per square meter. It was shown that the mean ambient field along a 6.4 m height above ground amounted to 8.29 kV/m for a field at ground level of 8 kV/m. This confirms that for the field tests modeled before, the effect of electric field nonuniformity due to the point discharge is insignificant.

From Tables I and II, it is realized that the rods struck by lightning are those having corona inception ground fields $\mathrm{E_{gci}}$ in the range 7.2–11.3 kV/m. The rod that is hit most frequently is the 19 mm rod. It is noted that there were two strikes to the 12.7 mm rod during triggered lightning. But the values of the ambient ground field during those experiments were not given. However, in [44], it was reported that successful launches at the site took place for ground fields in the range 4–13 kV/m. The fact that the sharp rod has never been hit, even for the much longer exposure of 48 years [45], could be accounted for by (14) since this rod has the lowest value of corona inception ground field and accordingly, the highest upward leader inception ground field.

Table II summarizes the results of lightning strikes to competing rods during the period 1994–1997.

The observation that the 51 mm rod has not been hit although its clean and dry corona inception ground field is as high as 17.8 kV/m may be explained by the fact that this relatively large diameter rod is more susceptible to surface roughness effects due to protrusions and water drops. In fact, a realistic surface roughness factor m of 0.33 [13] would bring the corona inception ground field of the 51 mm rod to 5.87 kV/m, which is practically identical to that of the 9.5 mm diameter rod, which also has never been struck. Experimental evidence in support of this explanation is shown in [8, Fig. 3] where it could be clearly seen that corona activity on the 51 mm rod was indeed more intense than that of the 19 mm rod, despite the larger diameter of the former.

We may therefore tentatively classify the six rods of Table II in two groups. The first group comprises the sharp rod and the 51 mm diameter rod, which may be referred to as "more prone to dc-corona formation," due to the sharp tip in one case and the susceptibility to surface contamination and water drops in the other. The other four rods by virtue of their corona onset fields of Table I, may be considered as "not prone to prolonged dc-corona formation." The fact that in nine natural and rocket-triggered strikes, the rods more prone to dc-corona were not struck clearly indicates the advantage of a rod that is less susceptible to corona under cloud charge fields.

To quantify this conclusion, consider the population mentioned before where the probability p corresponding to the two rods comprising the first corona prone group would be 1/3. If there was no physical difference in the strike mechanism between the two groups, the binomial distribution shows that in 9 strikes, the probability of at least one strike to this group would be 97%. The fact that no rod of this group was struck confirms the difference in the striking mechanisms of the two groups of rods and the advantage of the dc-corona free performance.

It should be emphasized that in [34], the space charge in the vicinity of the rod tip due to the cloud charge field, prior to negative leader descent, was not considered.

B. Proximity Effect of Adjacent Rods

A question has been raised with regard to the effect of lightning rod proximity in the New Mexico tests [33]. Here, we must distinguish between geometrical proximity and space charge shielding once an upward leader has been initiated.

As for the geometric effect, we used the charge simulation technique to determine the ambient field proximity factor defined as the ratio between the mean ambient fields at a rod position with and without the adjacent rod, as a function of the rod spacing. The results for 6.4 m rods are presented in Fig. 11 and show that for a rod spacing of 6 m, the presence of the adjacent rod reduces the mean ambient field by only 2.4%.

If, on the other hand, an upward leader is initiated first from a blunt rod, a sharp rod 6 m away would find its ability to produce a continuous upward leader suppressed in two ways: 1) by its own corona effect as explained before and 2) by the induced ambient field due to the blunt rod leader charge. We just considered a 1 m leader with a linear charge of 50 μC/m, the ambient field at the adjacent sharp rod location was reduced by 8.6 kV/m.

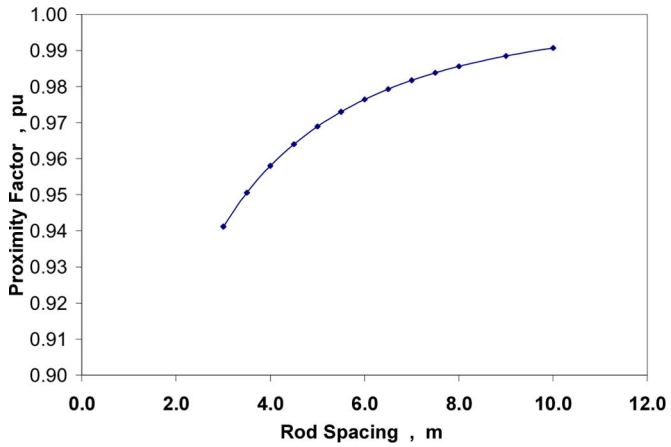

Fig. 11. Ambient field proximity factor due to an adjacent 6.4 m rod as a function of rod spacing.

The conclusion is that the sharp rod cannot produce an upward continuous leader in the presence of a blunt rod 6 m away that has already initiated its own leader.

VIII. Conclusion

1) Cloud charge field intensification at the tip of a slender lightning rod makes such a rod susceptible to corona formation in the absence of or prior to negative leader descent.
2) Corona onset of lightning rods due to cloud charge fields prior to leader descent is not restricted to tall rods but applies as well to the rods of practical height installed on top of tall structures.
3) In the absence of corona formation at the rod tip due cloud charge fields prior to negative leader descent, the rod diameter has no significant effect on upward connecting leader inception.
4) Laboratory tests to compare the performance of competing lightning rods would be meaningful only if performed with composite voltages comprising a dc component with a superimposed switching impulse.
5) A new analytical approach has been introduced to estimate the effect of corona space charge due to cloud charge fields prior to negative leader descent on continuous upward leader inception.
6) Under otherwise the same conditions, the effect of corona space charge produced by cloud charge fields on inhibiting upward leader inception will be more significant, the taller the rod, the higher the maximum ambient ground field will be, and the lower the corona inception field.
7) It has been found that for lightning rods of height in the 10 m range, the corona space charge prior to leader descent will have a limited effect on the attractive radius of a solitary rod but will have a determining effect on the competition of adjacent objects exposed to the same atmospheric conditions.
8) Based on the physics of electrical discharges, the characteristics of a non-self shielding air terminal were formulated.
9) Due to the effects of protrusions and water drops on large electrodes, a dc-corona-free rod, prior to the negative leader descent, with the smallest practical diameter is preferable.
10) The preferred rod slenderness ratio h/r is not a constant but varies with rod height, maximum ground field, and ambient relative air density.
11) For rods or masts of heights above flat ground in the tens of meters range, corona free performance prior to negative leader descent requires impractically large rod diameters which are moreover susceptible to deteriorated corona performance due to protrusions and water drops.
12) Both theory and field experience demonstrate the advantage of a lightning rod that is less prone to corona formation under cloud charge fields prior to negative leader descent.

References

[1] R. H. Golde, *Lightning Protection*. London, U.K.: Edward Arnold, 1973.
[2] M. A. Uman, *The Art and Science of Lightning Protection*. Cambridge, U.K.: Cambridge Univ. Press, 2008.
[3] R. B. Standler, "The response of elevated conductors to lightning," M.Sc. dissertation, Inst. Mining Technol., NM, May 1975.
[4] Les Renardières Group, "Long air gap discharges at Les Renardières: 1973 results," Electra, No. 23 and No. 35, Jul. 1972 and Jul. 1974.
[5] "Lightning Protector," U.S. Patent 1 266 175, May 14, 1918.
[6] G. N. Aleksandrov and G. D. Kadzov, "On increased effectiveness of lightning protection," *Elect. Technol. U.S.S.R.*, no. 1, pp. 75–82, 1987.
[7] F. A. M. Rizk, "Influence of rain on switching impulse sparkover voltage of large-electrode air gaps," *IEEE Trans. Power App. Syst.*, vol. PAS-95, no. 4, pp. 1394–1402, Jul. 1976.
[8] C. B. Moore, W. Rison, J. Mathis, and G. Aulich, "Lightning rod improvement studies," *J. Apppl. Meteorol.*, vol. 39, pp. 593–609, 2000.
[9] C. B. Moore, G. D. Aulich, and W. Rison, "Measurements of lightning rod responses to nearby strikes," *Geophys. Res. Lett.*, vol. 27, no. 10, pp. 1487–1490, May 15, 2000.
[10] *Standard for the installation of lightning protection systems*, Ed. NFPA 780, 2004.
[11] F. A. M. Rizk, "Modeling of lightning exposure of buildings and massive structures," *IEEE Trans. Power Del.*, vol. 24, no. 4, pp. 1987–1998, Oct. 2009.
[12] F. W. Peek, *Dielectric Phenomena in High Voltage Engineering*. New York: McGraw-Hill, 1929.
[13] P. S. Maruvada, *Corona Performance of High-Voltage Transmission Lines*. Baldock, Hertfordshire, U.K.: Research Studies Press, 2000.
[14] N. G. Trinh and J. B. Jordon, "Modes of corona discharges in air," *IEEE Trans. Power App. Syst.*, vol. PAS-87, no. 5, pp. 1207–1215, Feb. 1968.
[15] F. A. M. Rizk, "Switching impulse strength of air insulation: Leader inception criterion," *IEEE Trans. Power Del.*, vol. 4, no. 4, pp. 2187–2194, Oct. 1989.
[16] G. Carrara and L. Thione, "Switching surge strength of large air gaps: A physical approach," *IEEE Trans. Power App. Syst.*, vol. PAS-95, no. 2, pp. 512–524, Mar./Apr. 1976.
[17] L. Thione, "The electric strength of air gap insulation," in *Surges in High Voltage Networks*, K. Ragaller, Ed., 1979, pp. 165–205.
[18] H. Singer, H. Steinbigler, and P. Weiss, "A charge simulation method for calculation of high voltage fields," *IEEE Trans. Power App. Syst.*, vol. PAS-93, no. 5, pp. 1660–1668, Sep. 1974.
[19] *Insulation Coordination, Part 2: Application guide*, IEC Std. 60071-2, 1996.
[20] F. A. M. Rizk, "Modeling of lightning incidence to tall structures. Part I: Theory," *IEEE Trans. Power Del.*, vol. 9, no. 1, pp. 162–171, Jan. 1994.
[21] F. A. M. Rizk, "Modeling of transmission line exposure to direct lightning strokes," *IEEE Trans.*, vol. 5, no. 4, pp. 1983–1997, Oct. 1990.
[22] W. A. Chisholm and J. G. Anderson, "Lightning and Grounding," in *EPRI Transmission Line Reference Book*, 3rd ed. Palo Alto, CA: Elect. Power Res. Inst., 2003, ch. 6.

[23] H. R. Armstrong and E. R. Whitehead, "Field and analytical studies of transmission line shielding," *IEEE Trans. Power App. Syst.*, vol. PAS-87, no. 1, pp. 270–281, Jan. 1968.
[24] L. Dellera and E. Garbagnati, "Lightning stroke simulation by means of the leader progression model—Part 1: Description of the model and evaluation of exposure of free-standing stuctures," *IEEE Trans. Power Del.*, vol. 5, no. 4, pp. 2009–2022, Oct. 1990.
[25] N. I. Petrov and R. T. Waters, "Determination of the striking distance of lightning to earthed structures," *Proc. Roy. Soc.*, vol. 450, pp. 589–601, 1995, London A.
[26] P. Lalande, A. Bondiou-Clergerie, G. Bachiega, and I. Gallimberti, "Observations and modeling of lightning leaders," *C. R. Phys.*, vol. 3, pp. 1375–1392, 2002.
[27] T. Harada, Y. Aihara, and Y. Aoshima, "Influence of switching impulse wave shape on flashover voltages of air gaps," *IEEE Trans. Power App. Syst.*, vol. PAS-92, no. 3, pp. 1085–1093, May 1973.
[28] L. Zaffanella, "Switching Surge Performance," in *EPRI AC Transmission Line Reference Book*, 3rd ed. Palo Alto, CA: Elect. Power Res. Inst., 2003, ch. 5.
[29] C. Gary and B. Hutzler, "Laboratory simulation of the ground flash," *RGE*, no. 3, pp. 18–24, Mar. 1989.
[30] F. A. M. Rizk, "Critical switching impulse strength of long air gaps: Modelling of air density effects," *IEEE Trans. Power Del.*, vol. 7, no. 3, pp. 1507–1515, Jul. 1992.
[31] E. M. Bazelyan, N. L. Aleksandrov, Yu. P. Raiser, and A. M. Konchakov, "The effect of air density on atmospheric fields required for lightning initiation from a long airborne object," *Atmosph. Res.*, vol. 86, pp. 126–128, 2007.
[32] F. D'Alessandro, C. J. Kossmann, A. S. Gaivoronsky, and A. G. Ovsyannikov, "Experimental study of lightning rods using long sparks," *IEEE Trans.Dielectr. Electr. Insul.*, vol. 11, no. 4, pp. 638–649, Aug. 2004.
[33] N. L. Aleksandrov, E. M. Bazelyan, F. D'Alessandro, and Yu. P. Raizer, "Dependence of lightning rod efficacy on its geometric dimensions—A computer simulation," *J. Phys. D: Appl. Phys.*, vol. 38, pp. 1225–1238, 2005.
[34] M. Becerra and V. Cooray, "Time dependent evaluation of the lightning upward connecting leader inception," *J. Phys. D: Appl. Phys.*, vol. 39, pp. 4695–4702, 2006.
[35] N. L. Aleksandrov, E. M. Bazelyan, R. B. Carpenter, M. M. Drabkin, and Yu. P. Raizer, "The effect of coronae on leader initiation and development under thunderstorm conditions and in long air gaps," *J. Phys. D: Appl. Phys.*, vol. 34, pp. 3356–3266, 2001.
[36] N. L. Aleksandrov, E. M. Bazelyan, and Yu. P. Raizer, "The effect of a corona discharge on a lightning attachment," *Plasma Phys. Rep.*, vol. 31, no. 1, pp. 84–101, 2005.
[37] T. Watanabe, "Influence of preexisting DC voltage on switching surge flashover characteristics," *IEEE Trans. Power App. Syst.*, vol. PAS-87, no. 4, pp. 964–969, Apr. 1968.
[38] N. Knudsen and F. Iliceto, "Flashover tests on large air gaps with dc voltages and with switching surges superimposed on dc voltage," *IEEE Trans. Power App. Syst.*, vol. PAS-89, no. 5/6, pp. 781–788, May/Jun. 1970.
[39] C. Menemenlis and G. Harbec, "Behaviour of air insulating gap of dc system under impulse, dc and composite voltages," *IEEE Trans. Power App. Syst.*, vol. PAS-98, no. 6, pp. 2065–2075, Nov. 1979.
[40] "Overhead lines for HVDC transmission: Electrical performance of HVDC transmission lines," in *EPRI HVDC Reference Book*. Palo Alto, CA: Elect. Power Res. Inst., Jun. 2008.
[41] A. J. Eriksson, "An improved electrogeometric model for transmission lines shielding analysis," *IEEE Trans. Power Del.*, vol. 2, no. 3, pp. 871–886, Jul. 1987.
[42] C. T. R. Wilson, "The electric field of a thunder-cloud and some of its effects," in *Proc. Phys. Soc.*, London, U.K., 1925, vol. 37, pp. 32D–37D.
[43] F. A. M. Rizk, "Modeling of lightning incidence to tall structures, Part II: Applications," *IEEE Trans. Power Del.*, vol. 9, no. 1, pp. 172–193, Jan. 1994.
[44] P. Hubert, P. Laroche, A. Eybert-Berard, and L. Barret, "Triggered lightning in New Mexico," *J. Geoph. Res.*, vol. 89, no. 2, pp. 2511–2521, 1984.
[45] C. B. Moore, G. D. Aulich, and W. Rison, "The case for using blunt-tipped lightning rods as strike receptors," *J. Appl. Meteorol.*, vol. 42, pp. 984–993, 2003.

Farouk A. M. Rizk (LF'09), photograph and biography not available at the time of publication.